Physical Properties of Lyocell Fibers Spun from Different Solution-Dope Phases

DONG BOK KIM,[1] WHA SEOP LEE,[2] SEONG MU JO,[2] YOUNG MOO LEE,[1] BYOUNG CHUL KIM[1]

[1] Division of Chemical Engineering, Hanyang University, Haingdang, Seongdong, Seoul 133-791, South Korea

[2] Polymer Hybrid Center, Korea Institute of Science and Technology, Seoul 136-791, South Korea

ABSTRACT: The hydration number (n) of NMMO hydrates has a significant effect on the rheological properties and phase of the cellulose solutions in the hydrates. The physical properties of the lyocell fibers spun from the cellulose solutions in NMMO hydrates with different values of n were investigated relative to the phase of the solution dope. NMMO hydrate with $n = 1.1$ could not fully dissolve cellulose, resulting in a heterogeneous solution. NMMO hydrate with $n = 0.72$ produced a mesophase solution that exhibited a good spinnability. When NMMO hydrates with $n = 0.72$ and 1.0 were used, the lyocell fiber spun from 15 wt % solution dope gave higher tensile strength than that spun from 12 wt % solution dope. NMMO hydrate with $n = 1.0$ produced a lyocell fiber whose tensile strength was slightly affected by spin–draw ratio but the tensile strength of the lyocell fiber prepared from NMMO hydrate with $n = 0.72$ was monotonically increased with increasing spin–draw ratio. Further, the latter gave higher birefringence. The lyocell fiber spun from 15 wt % solution in NMMO hydrate with $n = 0.72$ produced finely fibrillated structures. When treated with sonic wave the lyocell fiber prepared from 15 wt % cellulose (DP_w 940) solution in NMMO hydrate with $n = 0.72$ yielded the most serious fibrillation on the fiber surface. © 2002 John Wiley & Sons, Inc. J Appl Polym Sci 83: 981–989, 2002

Key words: cellulose; NMMO hydrate; hydration number; physical properties; mesophase; spin–draw ratio

INTRODUCTION

Cellulose attracts much attention as plastics material because of its biodegradability and abundance on earth. The history of cellulose as regenerated man-made fibers, so-called rayon fiber, dates back to the early 1800s.[1–4] The bottleneck retarding technical breakthroughs concerning cellulose fiber has been to find out new solvent systems that can directly dissolve cellulose. However, N-methylmorpholine N-oxide (NMMO) hydrate has proved to be one of the most successful solvent systems for cellulose and has led to commercial production of cellulose fiber.[5–7] Cellulose fibers manufactured by direct dissolution are named as the lyocell fibers and have been commercialized since the 1980s. New technologies for manufacturing lyocell fibers have been developed by Courtaulds, Lenzing, Korea Institute of Science and Technology, and so on.[8–11] Lyocell fibers possess excellent physical properties, so they are readily finding applications in industrial fields as well as in the field of apparel.[12–15]

In solution spinning, the phase of spinning dope has a profound effect on the physical prop-

Correspondence to: B. C. Kim (bckim@email.hanyang.ac.kr).

erties of the resultant cellulose fibers. It is well recognized that the cellulose solutions in NMMO hydrates produce different phases according to the hydration number (n) of NMMO hydrate, concentration of cellulose, and temperature.[16–19] The cellulose solution yields the anisotropic phase only when $n < 1$. In this study, cellulose solutions in NMMO hydrates with different hydration numbers were prepared, and the physical properties of cellulose fibers spun from them are discussed in terms of hydration number, concentration, and molecular weight.

EXPERIMENTAL

Materials

The cellulose samples were supplied by ITT Rayonier, whose weight-average degree of polymerization (DP_w) was 940 (Rayonex-P) and 670 (Cellunia-F). They were dried at 80°C for 24 h prior to use. NMMO hydrate was purchased from Aldrich (Milwaukee, WI). The 49.6 wt % aqueous NMMO solution was condensed under vacuum at 100°C to produce 85–91 wt % NMMO hydrates. The water content in the condensed NMMO hydrates was measured by the method suggested by Fischer.[20] n-Propyl gallate (PG) was used as the antioxidant (0.5 wt % for cellulose).[21]
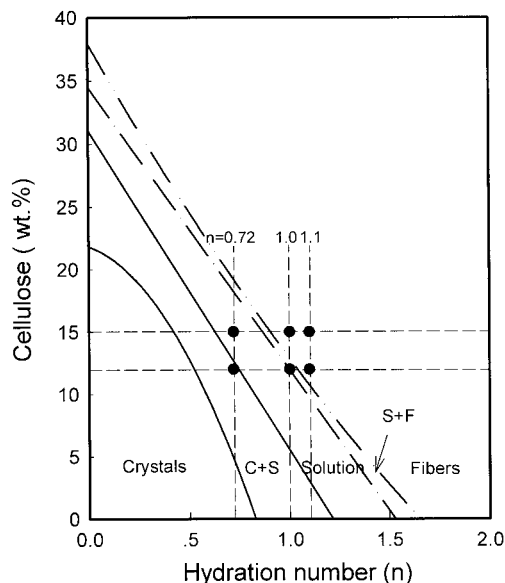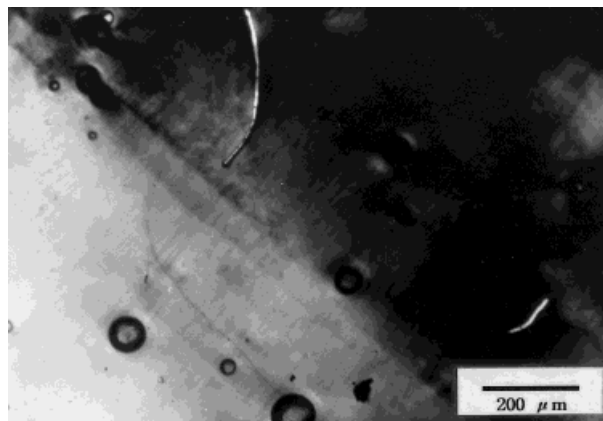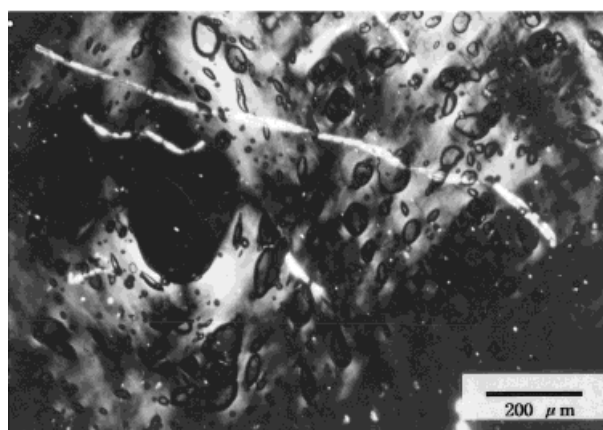
a)

b)

Figure 2 Photographs of 15 wt % cellulose solution in NMMO hydrate ($n = 1.0$) at 110°C: DP_w of cellulose is 670 (a) and 940 (b).

Preparation of Cellulose Fibers

Cellulose, PG, and NMMO hydrate were mixed simultaneously in the static rotary mixer for 10 min to yield a predope, and the cellulose solution in the NMMO hydrate was prepared by stirring the predope at 120–140°C for 40 min under vacuum.

The spinning experiment was carried out at 110°C by capillary nozzle, whose diameter was 0.7 mm and the length-to-diameter ratio of the nozzle was 30. The air gap was 200 mm, and distilled water was used as the coagulant at 20°C. The spin–draw ratios adopted were 28.5, 70, 128, and 170.

Measurement of Physical Properties

Rheological properties were measured by a Rheometrics dynamic spectrometer RDS 7700 (Rheo-
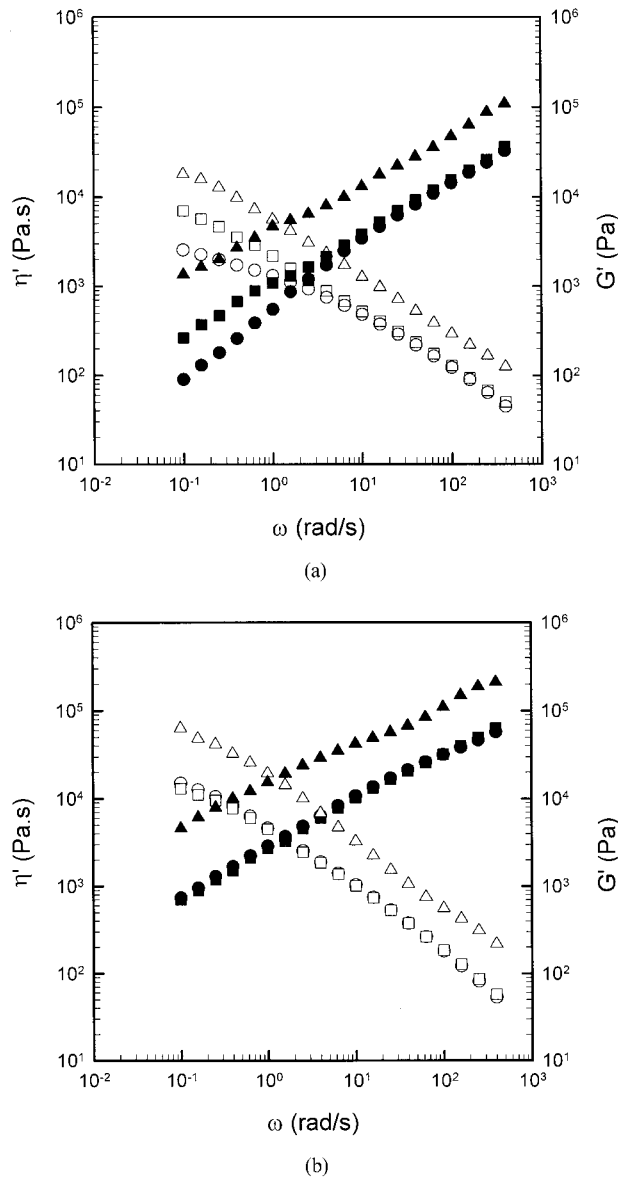
Figure 1 Cellulose dissolution in NMMO hydrate system.

Birefringence (Δn) was measured by a Nikon polarizing microscope (Type 104). Retardation (r in nm) was measured with quartz wedge and senarmont, and the diameter of fiber (d in nm) was measured by filar micrometer. Birefringence was calculated by the following equation:

$$\Delta n = \frac{r}{d}$$

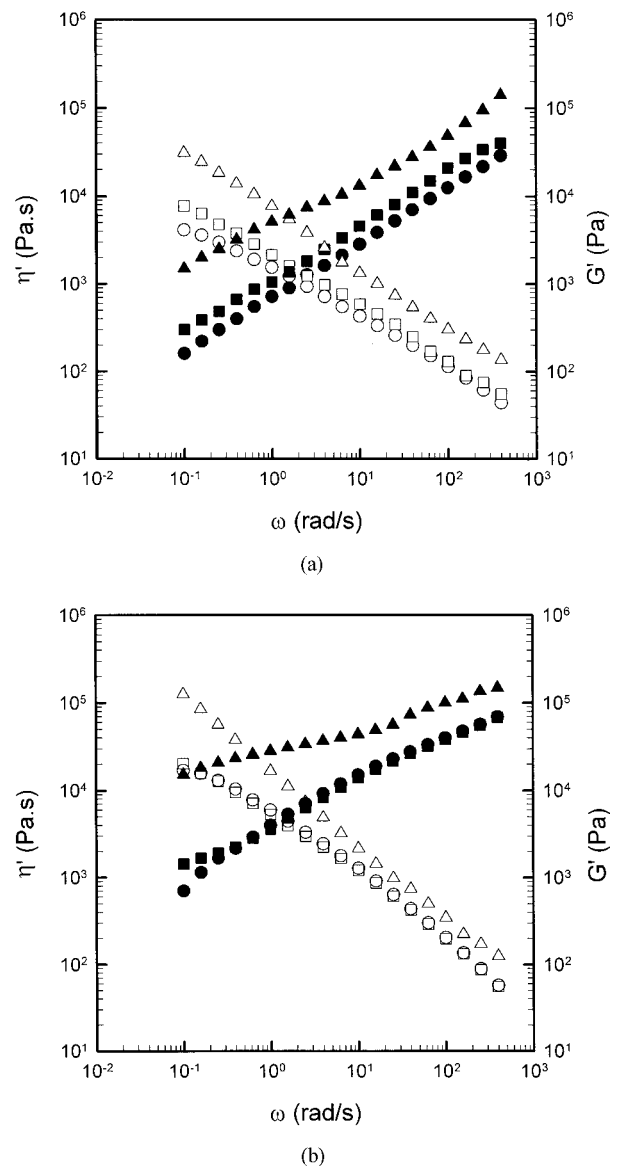The fibrillation experiment was performed by a Branson sonifier 450. A 15-mm-long cellulose fi-

Figure 3 Plot of η' and G' versus ω of 12 wt % cellulose solution in NMMO hydrates at 110°C: ○, ●, n = 1.1; □, ■, n = 1.0; and △, ▲, n = 0.72. Open symbol is η' and closed symbol is G'. DP_w of cellulose is 670 (a) and 940 (b).

metrics, Inc.) over the frequency range 0.1–500 rad/s at 110°C. The parallel plates of diameter of 25 mm were used, whose gap was 1.4 mm.

Tensile properties were measured by Instron (model 4464). Gauge length was 30 mm and crosshead speed was 10 mm/min. The average of 10 measurements was taken as data. The tensile-fractured surface of the fiber was observed by scanning electron microscope (SEM model S-510, Hitachi Ltd., Japan).

Figure 4 Plot of η' and G' versus ω of 15 wt % cellulose solution in NMMO hydrates at 110°C: ○, ●, n = 1.1; □, ■, n = 1.0; and △, ▲, n = 0.72. Open symbol is η' and closed symbol is G'. DP_w of cellulose is 670 (a) and 940 (b).
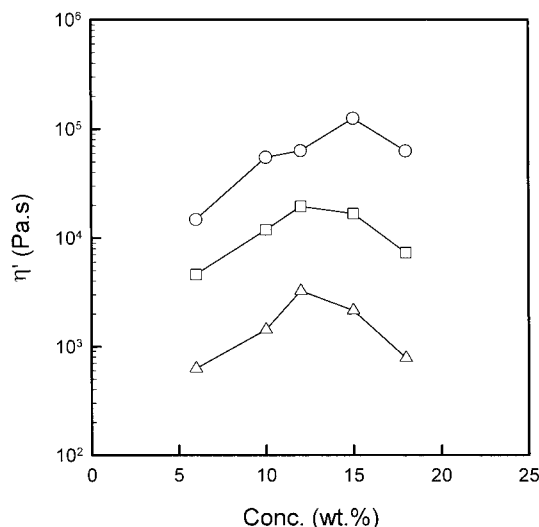
Figure 5 Concentration dependence of η' of cellulose (DP_w 940) solution in NMMO hydrate ($n = 0.72$) at 110°C for various frequencies: $\bigcirc$, $\omega = 0.1$; $\square$, $\omega = 1$; and $\triangle$, $\omega = 10$ rad/s.

ber was immersed in distilled water at 20°C for 10 min, then a strong sonic wave was radiated onto the surface of the fiber for 15 min.[17,22] The resultant fiber morphology was observed by scanning electron microscope (SEM model S-510; Hitachi, Ltd.).

RESULTS AND DISCUSSION

Effect of Hydration Number on the Solvating Power of NMMO Hydrates to Cellulose

NMMO dissolves cellulose because its N—O group can form hydrogen bonding. Among NMMO hydrates, anhydrous NMMO is known as the best solvent for cellulose. However, its actual applica-tion is limited because of its high melting temper-ature (T_m), 180°C.[23] Thus NMMO hydrates are generally used as the solvent for cellulose. The solvating power of NMMO hydrates is dependent on the value of n: if $n > 1.5$ it swells cellulose, and if $n > 2$ it becomes a nonsolvent. When the value of n is less than 1, the solvating power is improved with decreasing the value.
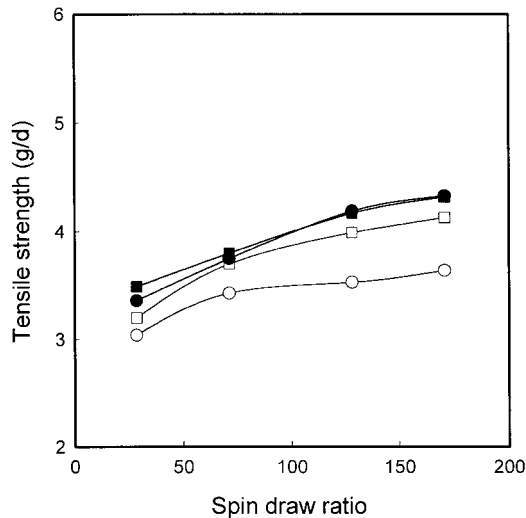
Figure 1 shows the phase diagram of cellulose solutions in NMMO hydrates.[24] Anhydrous NMMO dissolves cellulose up to 35 wt %. How-ever, NMMO hydrate with $n = 1.1$ leaves undis-solved microfibrils even at 15 wt %. This figure further reveals that the cellulose solution system in NMMO hydrates comprises various phases ac-cording to the concentration and the value of n. At a given concentration, for example, at a concen-tration in between 10 and 15 wt % in the diagram, the cellulose–NMMO hydrate system produces a transition with increasing hydration number[7,24]: crystals $\rightarrow$ crystals + solution $\rightarrow$ solution $\rightarrow$ fibers + solution $\rightarrow$ fibers. The crystal region results from the existence of anhydrous NMMO crystal. The S + F region contains some undissolved cel-lulose fibrils, and cellulose is only swollen without being dissolved in the fiber region.[25]

Figure 2 shows an optical microphotograph of morphology of 15 wt % solution of cellulose (DP_w 670 and 940) in NMMO monohydrate ($n = 1.0$). Figure 2(a) (DP_w 670) shows that some undis-solved cellulose microfibrils exist in the solution. Figure 2(b) (DP_w 940) clearly shows that the amount of microfibrils is increased when the mo-lecular weight of cellulose is increased. This agrees with the phase diagram; the vertical dash line ($n = 1.0$) indicates that only the 12–13 wt % cellulose solutions are completely dissolved, and some microfibrils remain undissolved if the con-centration is higher than 15 wt %.
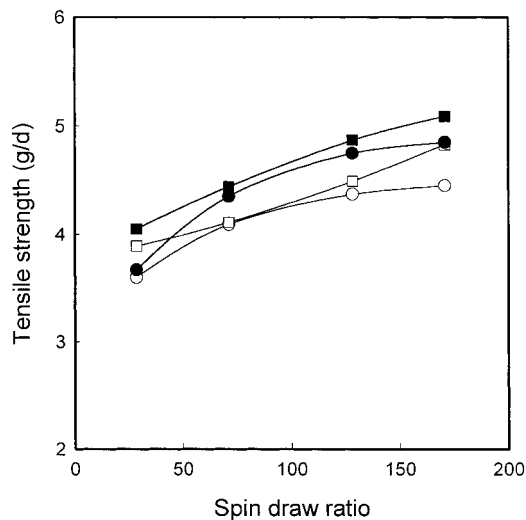
Table I   Spinnability of Cellulose Solutions in NMMO Hydrate at 110°C

DP_w	Concentration (wt %)	Phase and Spinnability[a]		
		$n = 1.1$	$n = 1.0$	$n = 0.72$
670	12	I, PS	I, S	A, S
	15	I, PS	I, (PS or S)	A, S
940	12	I, PS	I, S	A, S
	15	I, NS	I, PS	A, S

[a] I, isotropic phase; A, anisotropic phase; S, spinnable; PS, poor spinnable; NS, nonspinnable.
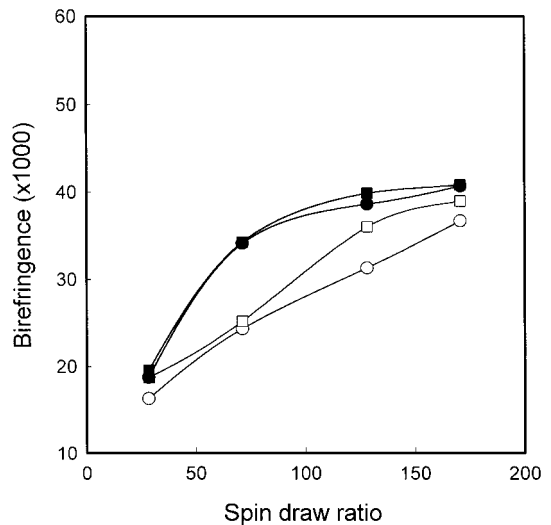
On the rheological principle, disappearance of the lower Newtonian flow region is indicative of the existence of heterogeneity in the solution. The heterogeneity of 12 wt % cellulose (DP_w 670) solution in the NMMO hydrate with $n = 0.72$ results from the development of the mesophase through spontaneous molecular ordering. When $n = 1.0$, the cellulose solution produces an isotropic phase. On the other hand, the heterogeneous characteristics of the cellulose solution for $n = 1.1$ seem to originate from free water in the NMMO hydrate. That is, some cellulose microfi-

(a)

(b)

Figure 6 Plot of tensile strength of cellulose fiber versus spin–draw ratio: ○, ●, $n = 1.0$ and □, ■, $n = 0.72$. Open symbol is 12 wt % and closed symbol is 15 wt %. DP_w of cellulose is 670 (a) and 940 (b).
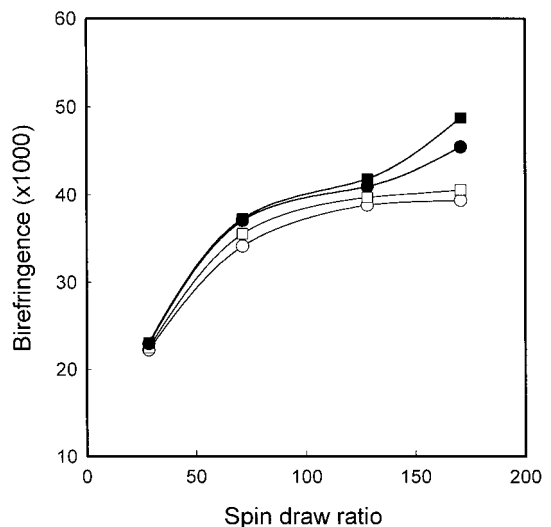
Rheological Properties of Solution Dope of Cellulose in NMMO Hydrates

Figures 3 and 4 present the rheological properties of 12 and 15 wt % cellulose solutions, respectively, in NMMO hydrates with various values of n (refer to the black mark in Fig. 1). In the figures, (a) measures cellulose with DP_w 670 and (b) measures cellulose with DP_w 940. Over the frequency range 0.1–500 rad/s all the cellulose solutions give rise to a low-shear range shear thinning, which is least noticeable with $n = 1.1$ and most noticeable with $n = 0.72$.

(a)

(b)

Figure 7 Plot of birefringence of cellulose fiber versus spin–draw ratio of cellulose fiber. DP_w of cellulose is 670 (a) and 940 (b). Symbols are the same as those in Figure 6.
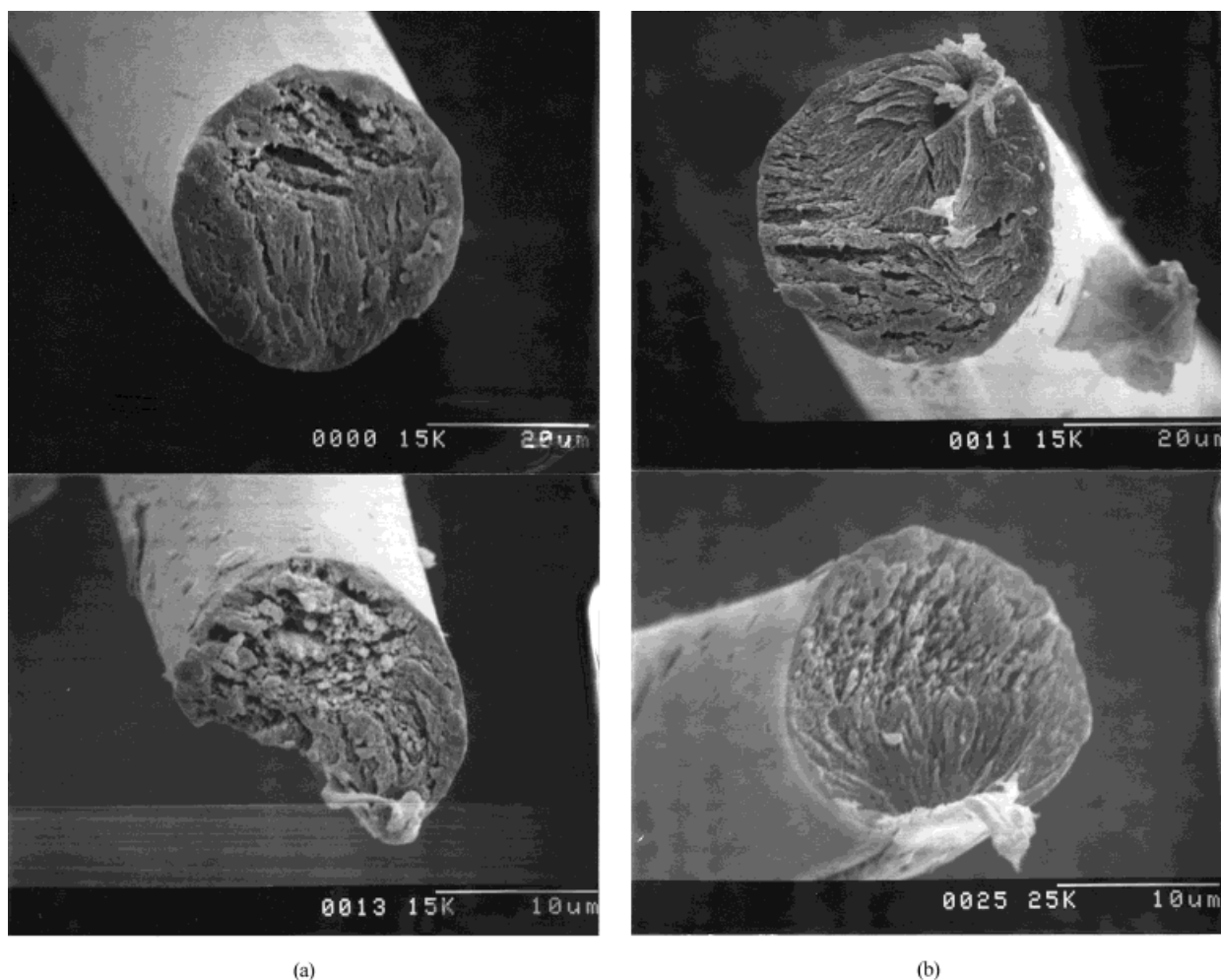
(a)   (b)

Figure 8   Effect of hydration number (n) in NMMO hydrate on the morphology of cellulose fiber at the spin–draw ratios 28.5 and 170. DP_w of cellulose is 670 and dope concentration is 12 wt %. (a) $n = 1.0$ and (b) $n = 0.72$.

brils exist in the solution because of poor solubility.

These characteristic features in the rheological responses become clearer as the molecular weight of cellulose increases from DP_w 670 to DP_w 940 (Fig. 3). In addition, the 15 wt % cellulose solution in NMMO hydrate with $n = 0.72$ more readily produces the mesophase at the higher molecular weight of cellulose (Fig. 4). However, the cellulose solutions in NMMO hydrate with $n = 1.0$ and 1.1 do not exhibit notable differences in rheological properties because the effect of undissolved microfibrils of cellulose is superimposed on them.

In isotropic polymer solutions both viscosity and elasticity are generally increased with increasing concentration and molecular weight of the polymer. The cellulose solutions in NMMO hydrates with $n = 1.0$ and 1.1 (in Figs. 3 and 4)

indicate that an increase in both concentration and molecular weight of cellulose increases both dynamic viscosity and storage modulus.

On the other hand, in anisotropic polymer solutions a critical concentration appears, above which a further increase in concentration reduces viscosity that results from spontaneous ordering of polymer chains up to the saturation concentration at which a partial solidification occurs.[26–33]

Figure 5 presents a plot of the dynamic viscosity of cellulose (DP_w 940) solutions in NMMO hydrate with $n = 0.72$ at 110°C. The critical concentration appears in the concentration range of 12–15 wt %, which is slightly decreased with increasing frequency. The decrease in critical concentration results from easier orientation of cellulose molecules at a higher shear rate.
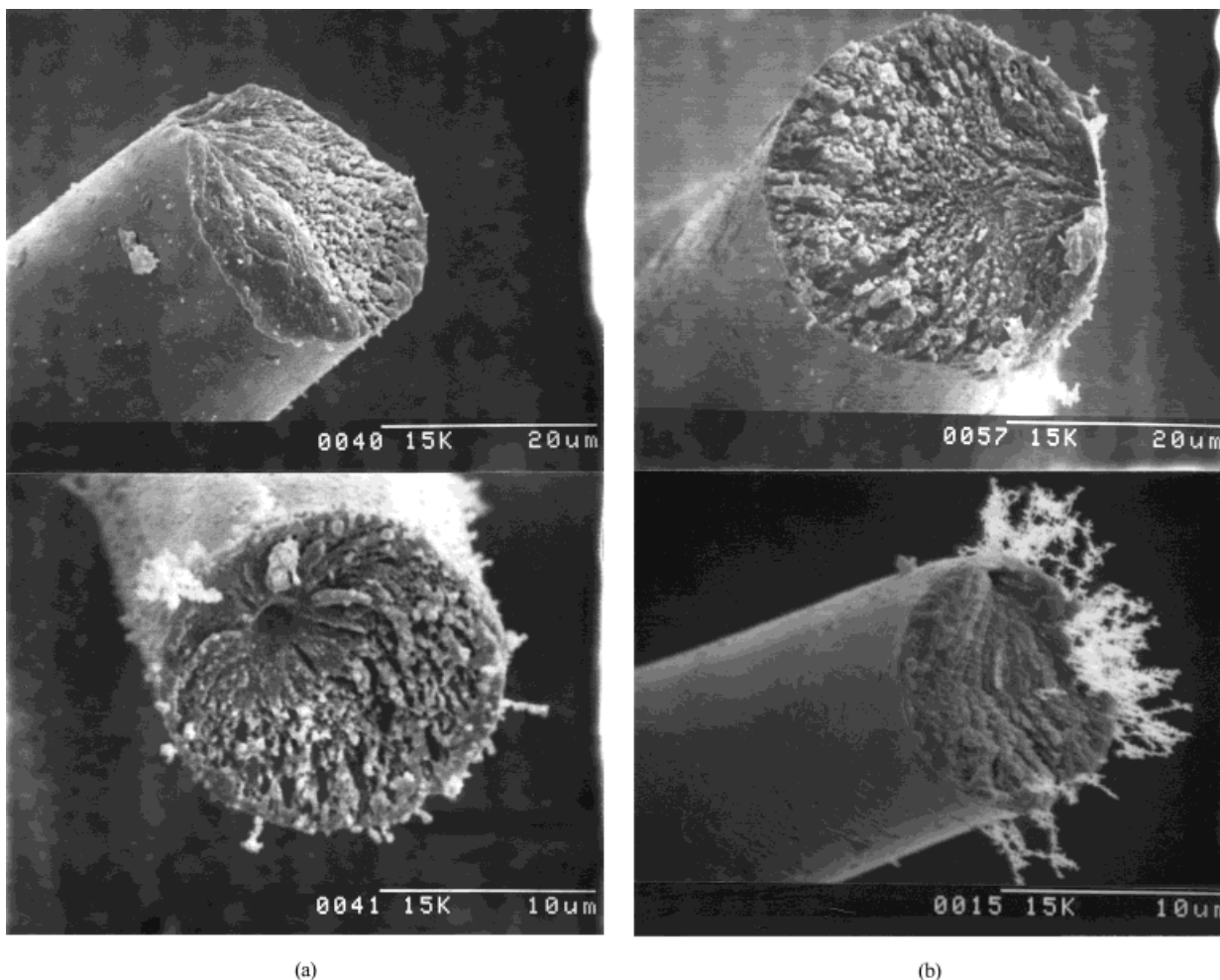
Figure 9 Effect of molecular weight of cellulose on the morphology of cellulose fiber at the spin–draw ratios 28.5 and 170. n is 0.72 and dope concentration is 15 wt %. (a) DP_w 670 and (b) DP_w 940.

Spinnability of Cellulose Solutions in NMMO Hydrates at 110°C

Observation of the spinning process of cellulose solutions in NMMO hydrates reveals the result summarized in Table I. The cellulose solution in NMMO hydrate with $n = 0.72$ takes on a honey-like color, whereas that in NMMO hydrate with $n = 1.1$ takes on a slightly opaque milky color. All the cellulose solutions in NMMO hydrate with $n = 1.1$ give very poor spinnability as the result of a serious break of spinline. Hence, we investigate the lyocell fibers spun from 12 and 15 wt % cellulose solutions in NMMO hydrates with $n = 0.72$ (anisotropic solution) and 1.0 (isotropic solution).

Physical Properties of Lyocell Fiber

Figure 6 presents spin–draw ratio–dependent tensile strength of lyocell fibers spun from differ-

ent solution-dope phases. As expected the tensile strength increases as the spin–draw ratio is increased because of the increases in molecular orientation by elongational stress.[17,34] In addition, the value of n has a significant effect on the tensile strength. As shown in Figure 6(a) the lyocell fiber spun from the cellulose solution in NMMO hydrate with $n = 0.72$ exhibits higher tensile strength than that spun from the cellulose solution in NMMO hydrate with $n = 1.0$.

The lyocell fibers prepared by using cellulose with higher molecular weight (DP_w 940) give a similar result, as shown in Figure 6(b). As in Figure 6(a) the tensile strength is increased with increasing the spin–draw ratio. Although the tensile strength of the lyocell fiber spun from the cellulose solutions in NMMO hydrate with $n = 1.0$ is only slightly affected by spin–draw ratio, that of the lyocell fiber spun from the cellulose

solutions in NMMO hydrate with $n = 0.72$ is monotonically increased with increasing spin–draw ratio. This results from the fact that the mesophase gives rise to much enhanced orientation of molecules during spinning.[17]

Figure 7 shows variation of birefringence of the lyocell fiber spun from 12 and 15 wt % cellulose solutions in NMMO hydrates with $n = 0.72$ and 1.0. Figure 7(a) measures cellulose with DP_w 670 and Figure 7(b) measures cellulose with DP_w 940. In general birefringence is increased as the spin–draw ratio is increased, and higher birefringence is observed at lower values of n. In addition, birefringence is increased with increasing concentration and molecular weight of cellulose, as shown in Figure 7(b).

Figures 8 and 9 show microphotographs of the tensile-fractured cross section of lyocell fiber spun from different solution-dope phases. As the spin–draw ratio is increased from 28.5 to 170, the diameter of the lyocell fiber spun from 12 wt % cellulose (DP_w 670) solution is reduced from 36 to 18 μm (Fig. 8). An increase of molecular orientation with drawing is well evidenced by the existence of microfibrils on the tensile-fractured surface.[17] In the case of the lyocell fiber spun from 12 wt % cellulose solutions, the effect of the value of n on the formation of the microfibrils is not so noticeable, as shown in Figure 8.

On the other hand, in the case of the lyocell fiber spun from 15 wt % cellulose solution with $n = 0.72$, the effect of the value of n on the formation of the microfibrils is significant, as shown in Figure 9. This fiber contains a profusion of microfibrils. Even at a low spin–draw ratio the fiber produces finely fibrillated structures if the molecular weight of cellulose is high. To obtain more detailed data on the microfibrils, the lyocell fiber is treated with sonic wave.[22] A notable fibrillation on the fiber surface is brought about, as shown in Figure 10. The diameter of the microfibrils is affected by the value of n of NMMO hydrate. In the case of $n = 1.0$ the diameter of microfibrils ranges from 1 to 2.5 μm, whereas in the case of $n = 0.72$ the diameter of microfibrils ranges from 0.3 to 1.5 μm. This suggests that the lyocell fiber spun from mesophase yields microfibrils with smaller diameters.

CONCLUSIONS

The effect of the physical properties of spinning dope on the mechanical properties of lyocell fiber
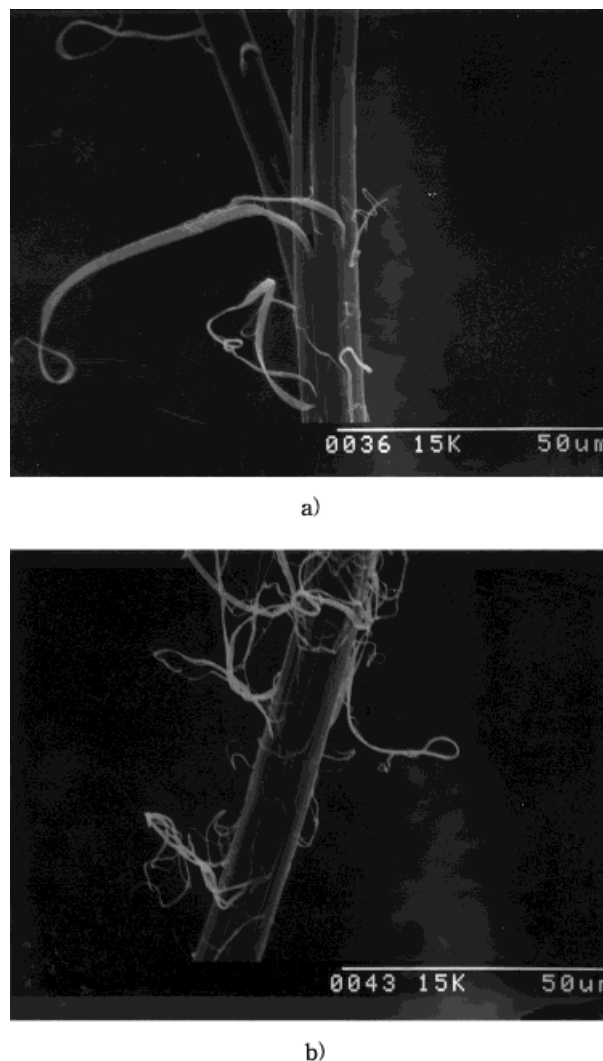

Figure 10   Effect of hydration number (n) of NMMO hydrate on the fibrillation of cellulose fiber after treatment with an ultrasonic generator for 15 min. DP_w of cellulose is 940, concentration is 15 wt %, and spin–draw ratio is 170. (a) $n = 1.0$ and (b) $n = 0.72$.

was investigated. The cellulose solutions in NMMO hydrate with $n = 1.1$ contained some undissolved cellulose fibrils, resulting in poor spinnability. The cellulose solutions in NMMO hydrate with $n = 0.72$ developed mesophase at the spinning temperature, which was helpful to spinnability and molecular orientation. In addition, the phase of the spinning dope of the lyocell fiber had a profound influence on the thickness of the resultant microfibrils. These results would provide the fundamental basis for the manufacturing processes of lyocell fibers that use NMMO hydrate as a direct solvent.

REFERENCES

1. Audemars, G. Brit. Pat. 283, 1855.
2. Chardonnet, H. B. Fr. Demande 165,349, 1884.
3. Despaissis, L. H. Fr. Demande 203,741, 1890.
4. Cross, C. F.; Bevan, E. J.; Beadle, C. Brit. Pat. 8700, 1892.
5. Johnson, D. L. Brit. Pat. 1,144,048, 1967.
6. Franks, N. E.; McCorsley, C. C.; Varga, K. U.S. Pat. 4,145,532, 1979.
7. Turbak, A. F.; Hammer, R. B.; Davies, R. E.; Hergert, H. L. Chem Technol 1977, 11, 702.
8. McCorsley, C. C. U.S. Pat. 4,246,221, 1981.
9. Michels, C.; Maron, R.; Berghof, K. U.S. Pat. 5,417,909, 1995.
10. Michels, C.; Maron, R.; Taeger, E. Lenzinger Berichte 1994, 9, 57.
11. Lee, W. S.; Jo, S. M.; Kang, H. J.; Kim, D. B.; Park, C. S. U.S. Pat. 5,584,919, 1996.
12. Loubinoux, D.; Chaunis, S. Text Res J 1987, 61.
13. Navard, P.; Haudin, J. M. Polym Proc Eng 1985, 3, 291.
14. Chanzy, H.; Paillet, M.; Hagege, R. Polymer 1990, 31, 400.
15. Chun, S. W.; Jo, S. M.; Lee, W. S.; Kim, J. D. J Kor Fiber Soc 1992, 29, 44.
16. Chanzy, H.; Peguy, A.; Chaunis, S.; Monzie, P. J Polym Sci Polym Phys Ed 1980, 18, 1137.
17. Kim, D. B.; Lee, W. S.; Kim, B. C.; Jo, S. M.; Park, J. S.; Lee, Y. M. Polymer (Korea) 1998, 22, 231.
18. Kim, D. B.; Lee, W. S.; Jo, S. M.; Lee, Y. M.; Kim, B. C. Polym J to appear.
19. Navard, P.; Haudin, J. M. Br Polym J 1980, 12, 174.
20. Fischer, K. Angew Chem 1935, 48, 394.
21. Loubinoux, D.; Chaunis, S. Lenzinger Berichte 1985, 59, 105.
22. Mortimer, S. A.; Peguy, A. A. J Appl Polym Sci 1996, 60, 305.
23. Chanzy, H.; Nawrot, S.; Peguy, A.; Smith, P.; Chevalier, J. J Polym Sci Polym Phys Ed 1982, 20, 1909.
24. Franks, N. E.; Varga, J. K. U.S. Pat. 4,196,282, 1980.
25. Chanzy, H.; Noe, P.; Paillet, M.; Smith, P. J Appl Polym Sci Appl Polym Symp 1983, 37, 239.
26. Flory, P. J. Adv Polym Sci 1984, 59, 1.
27. Flory, P. J. Proc R Soc London Ser A 1956, 234, 73.
28. Flory, P. J. Macromolecules 1978, 11, 1141.
29. Navard, P.; Haudin, J. M.; Dayan, S.; Sixon, P. J Polym Sci Polym Lett Ed 1981, 19, 379.
30. Krigbaum, W. R.; Hekemi, H.; Ciferri, A.; Conio, G. Macromolecules 1985, 18, 973.
31. Bianchi, E.; Ciferri, A.; Conio, G.; Cosani, A.; Terbojevich, M. Macromolecules 1985, 18, 646.
32. Patel, D. L.; Gilbert, R. D. J Polym Sci Polym Phys Ed 1981, 19, 1231.
33. Dave, V.; Glasser, W. G. J Appl Polym Sci 1993, 48, 683.
34. Mortimer, S. A.; Peguy, A. A. J Appl Polym Sci 1996, 60, 1747.